Bioorganic Chemistry 89 (2019) 102971

Contents lists available at ScienceDirect

Bioorganic Chemistry

journal homepage: www.elsevier.com/locate/bioorg

Discovery of novel (+)-Usnic acid derivatives as potential anti-leukemia agents with pan-Pim kinases inhibitory activity

Shuxiang Wang, Jie Zang, Min Huang, Lihong Guan, Kun Xing, Jian Zhang, Dan Liu*, Linxiang Zhao*

Key Laboratory of Structure-Based Drugs Design & Discovery of Ministry of Education, Shenyang Pharmaceutical University, Shenyang 110016, China

ARTICLE INFO

Keywords:
Usnic acid derivatives
Flavanone
Leukemia
Pim inhibition

ABSTRACT

Usnic acid (UA) is the main secondary metabolite isolated from lichens, with moderate anticancer activity. A small group of (+)-UA derivatives characterized with flavanone moiety was designed and synthesized, and their anticancer activities were evaluated in leukemia cells. It was demonstrated that (+)-UA derivatives **6a–6g** inhibited the proliferation of leukemia cells HL-60 and K562 with low micromolar IC_{50} values. Mechanisms of action were investigated to find that **6g** induced apoptosis in HL-60 and K562 cell lines, and affected the expression of MNK/eIF4E axis-related proteins, such as Mcl-1, p-eIF4E, p-4E-BP1. Finally, kinase inhibition assay suggested **6g** was a potential inhibitor of pan-Pim kinases. Meanwhile, the blocking of phosphorylation of BAD and 4E-BP1 by **6g**, together with the proposed binding mode of **6g** with Pim-1 further confirmed its Pim inhibition effects. Our finding provides the sight towards the potential mechanism of (+)-UA derivatives **6g** as anti-leukemia agents.

1. Introduction

There has always been unshrinkable interest in discovering bio-active small molecules with novel scaffolds to fulfill the unmet need for drug leads originated from natural products [1]. Usnic acid (UA, two isomers *i.e.* **1** and **2**, Fig. 1), a secondary metabolite isolated from the globally distributed lichens, is especially abundant in *Alectoria*, *Cladonia*, *Usnea*, *Lecanora*, *Ramalina* and *Evernia* [2]. (+)-UA (**1**) gets more attention than (-)-UA (**2**) as it exhibits greater potency and a wider range of biological activities including antibiotic, antiviral, anti-inflammatory and anti-proliferative activities [3,4]. UA contains a unique dibenzofuran scaffold, which is rare but could be seen in other natural products like (-)-Cercosporamide (**3**) [5], UA amide (**4**) [6] as well as synthetic active compounds CGS-34043 (**5**) [7], as shown in Fig. 1. Cercosporamide, similar to UA in scaffold, was recently reported as a novel MNK1/2 kinase inhibitor with both *in vitro* and *in vivo* activity [5]. Structure differences between two compounds occur at three positions: the presence of methyl group at C-8 or not, the carbamoyl group rather than acetyl at C-6 and the opposite methyl configuration at C (9b).

Structure modification efforts focused on the C-2 acetyl group of UA have been pursued to improve its various bioactive activities [4,8–10]; its molecular mechanism of anticancer activity was involved in several reports, including suppressing VEGFR2-mediated Akt and ERK1/2 signaling pathways in breast tumor [11], induction of cell cycle arrest and apoptosis in lung carcinoma A549 cells [12]. Recent work by Zuo et al. demonstrated that UA inhibits tumor growth in MCF-7 tumor-bearing mice without significant toxicity and induces apoptosis via an ROS-dependent mitochondrial pathway [13]. However, its potential target of the anticancer effects and structure modifications at other sites are yet to be explored. Our previous study has demonstrated that UA exhibits the abilities of inhibiting growth and inducing apoptosis in human myeloid leukemia cells, but it only showed moderate anti-proliferative activity against HL-60 and K562 cells [14]. Hence, there is a pressing demand to enhance the potency of UA against leukemia cells by structure modification and verify the potential target of the corresponding derivatives. As mentioned above, (+)-UA gets more attention than (-)-UA as it exhibits greater potency and a wider range of biological activities, and our research is also focused on (+)-UA development.

Flavanone represents a privileged skeleton in synthetic compounds and natural products [15,16]. There has been growing evidence to support that compounds containing this skeleton showed moderate to high anticancer activities against various cancer cell lines. In our efforts to improve the anticancer potency of (+)-UA, a different modification site at C-6 acetyl and C-7 hydroxyl group rather than the C-2 acetyl

* Corresponding authors.
E-mail addresses: sammyld@163.com (D. Liu), linxiang.zhao@vip.sina.com (L. Zhao).

https://doi.org/10.1016/j.bioorg.2019.102971
Received 26 January 2019; Received in revised form 20 April 2019; Accepted 30 April 2019
Available online 02 May 2019

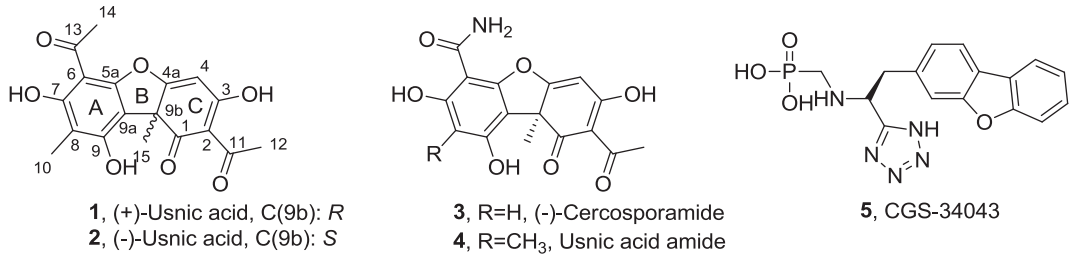

Fig. 1. Structures of representative agents with dibenzofuran scaffold including UA, Cercosporamide, UA amide and CGS-34043.

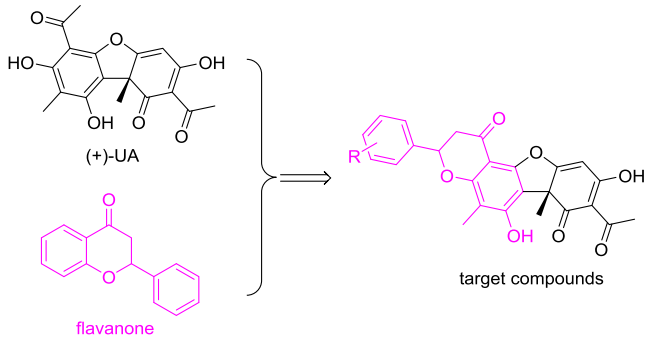

Fig. 2. Design of novel (+)-UA derivatives containing a flavanone moiety.

group was employed. We successfully introduced flavanone into (+)-UA to obtain a series of novel analogues of (+)-UA (Fig. 2). Herein, we present the design, synthesis and biological evaluation of those (+)-UA derivatives, which bear the flavanone moiety in their structures. The target compounds synthesized and evaluated for the biological activities are in the form of a racemic mixture.

2. Results and discussion

2.1. Chemistry

Previous studies provide a plausible synthetic route to prepare chalcones, flavonols, dihydroflavonols and flavones after ring C was protected by forming pyrazole with phenylhydrazine [17,18]. The construction of flavanone structure is usually achieved through two steps *i.e.* condensation of 2-hydroxyacetophenone with different aromatic aldehydes at mild condition, followed by refluxing obtained *o*-hydroxychalcones in the presence of acid or base to afford flavanone [19]. In our earlier study to synthesize derivatives of UA at C-2 position, we noticed that a different reactive activity existed between acetyl groups at C-2 and C-6, consistent with the literature reported [20]. Therefore, with ring C unprotected, (+)-UA was attempted to condense with various substituted benzaldehydes within one-step in alkaline condition to give derivatives **6a–6g** in moderate yields (Scheme 1).

2.2. Biological evaluation

2.2.1. In vitro antiproliferative activity

The antiproliferative effects of target compounds **6a–6g** were tested on two human leukemia cell lines (acute promyelocytic leukemia cells HL-60 and chronic myelogenous leukemia cells K562). (+)-UA, the parent compound, was used as positive control. The IC_{50} values for all the tested compounds are shown in Table 1. It was found that the introduction of flavanone moiety resulted in about 4-fold improvement on potency compared with (+)-UA, which exhibited IC_{50} of 10.32 μM and 10.49 μM against HL-60 and K562 cells, respectively. 4-fluoro substituted derivative **6c** and 4-chloro substituted derivative **6g** showed the best activities against both cells with IC_{50} value between 2.64 and 2.82 μM. Generally, different substituents caused little change in potency, except that electron-donating group methoxyl seemed to be discriminated at the *para* position; therefore, **6g** was selected as the representative derivative to conduct further mechanistic study.

Table 1
Structures of (+)-UA derivatives 6a–6g and their antiproliferative effects against leukemia cells.

Compd.	R	IC_{50} (μM)[a]	
		HL-60	K562
6a	H	2.79 ± 0.38	4.78 ± 0.29
6b	3-NO_2	2.23 ± 0.55	3.55 ± 0.59
6c	4-F	2.71 ± 0.78	2.82 ± 0.44
6d	4-OMe	3.25 ± 0.35	6.20 ± 0.63
6e	4-Br	2.70 ± 0.49	3.55 ± 0.62
6f	3-Cl	2.15 ± 0.35	3.93 ± 0.38
6 g	4-Cl	2.64 ± 0.31	2.70 ± 0.17
(+)-UA	–	10.32 ± 1.03	10.49 ± 0.60

[a] Determined using Typan blue exclusion assay after incubation with indicated compound for 72 h. Data are shown as mean ± SD from three independent assays.

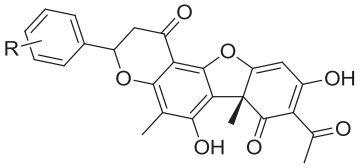

2.2.2. *6g induced leukemia cell lines apoptosis*

Induction of apoptosis has been recognized as a possible mechanism of action underlying the cytotoxicity of UA and its derivatives [21]. In this regard, we next investigated the effect of potent (+)-UA derivative **6g** on apoptosis-inducing with PI staining in HL-60 and K562 cells. In fact, K562 cells are highly tolerant to almost all drugs compared to HL-60 cells. Due to the phenomenon of tolerance and the differential level of expression of the potential targets of this series of compounds in both

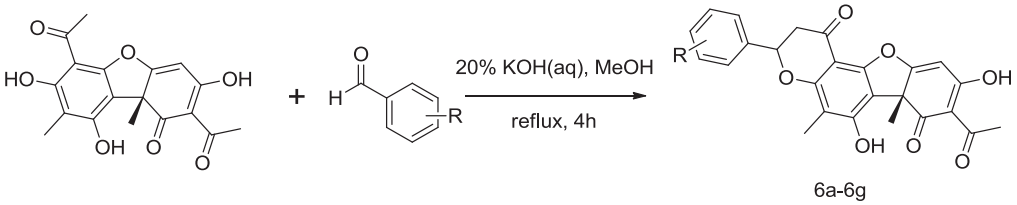

Scheme 1. Synthetic route for target compounds 6a–6g.

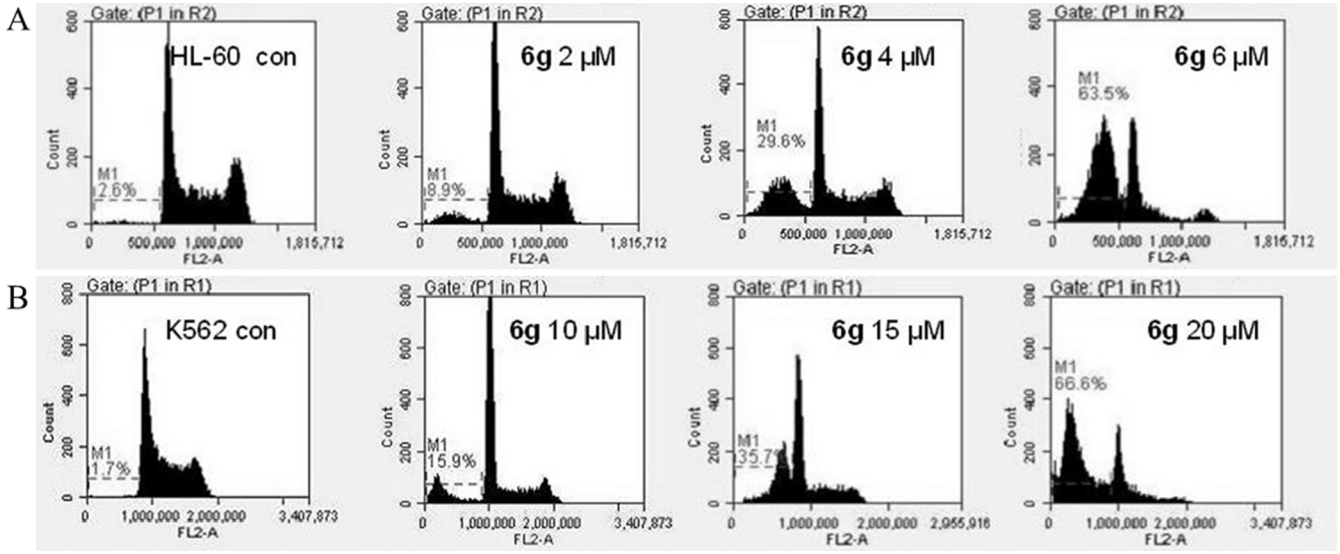

Fig. 3. Flow cytometric analyses of 6g on (A) HL-60 and (B) K562 cell lines determined by FACS analysis after staining with PI. HL-60 cells were treated with 6g at the indicated concentrations for 18 h; K562 cells were treated with 6g at the indicated concentrations for 48 h. The hypodiploid apoptotic peak (sub-G1) was determined by flow cytometry after staining with PI. Con, control; M1, apoptotic cells in sub-G1 phase.

cells, compound 6g showed poor apoptosis induction ability at low concentrations in K562 cells (data not shown). On this account, HL-60 cells were treated with 2, 4, 6 μM of **6g** for 18 h and K562 cells were treated with 10, 15, 20 μM of **6g** for 48 has shown in Fig. 3.

Apoptotic cells were given as the ratio of sub-G1 phase cells, **6g** led to a dose-dependent accumulation of apoptotic cells in both cell lines. The data demonstrated that **6g** exhibited significant apoptosis occurrence in HL-60 cells at 6 μM (63.5%) in comparison with control cells (2.6%). K562 cells were less sensitive to **6g**, and the apoptosis could only be observed at a prolonged period at 48 h and increasing concentrations. These results suggested that **6g** was a potent apoptosis inducer in leukemia cells.

2.2.3. *Mechanism studies of the apoptosis effects triggered by **6g***

To further elucidate the role of (+)-UA derivatives **6g** in apoptosis-related pathways, apoptosis related proteins were detected with Western blot assay. The caspase family proteins, including caspase-9, caspase-8 and caspase-3, as well as known downstream substrates such as PARP, play vital roles in apoptosis process [22]. Those proteins were analyzed in **6g**-treated HL-60 cells. It was found that **6g** led to the cleavage and activation of PARP and caspase-3/9, while the level of Bcl-2 remained unaltered (Fig. 4). Significantly, Mcl-1, an anti-apoptosis protein, was sharply decreased upon treatment of **6g** in HL-60 cell lines, suggesting a dominating role in **6g**-induced apoptosis. These results revealed that endogenic (mitochondrial) pathways participated in the apoptosis process. Meanwhile, the cleavage of caspase-8 was not obvious, which demonstrated that extrinsic pathways may not participate in the apoptosis process induced by **6g**.

2.2.4. *6g inhibited the phosphorylation of eIF4E*

MEK/MAPK/MNK and PI3K/Akt/mTOR signaling pathways converge at the nexus of eIF4E and promote cell survival and translation process of many oncogenic proteins such as Mcl-1 [23], we next studied the potential effects of **6g** on those related pathways. As can be seen from Figs. 5 and 6**g** could block the phosphorylation of eIF4E, a key component in translation machinery, without affecting upstream ERK, which was quite similar with the effect of Cercosporamide. These data suggested **6g** might function as MNK1/2 kinase inhibitors [4]. However, they failed to show any activity towards MNK1/2 kinase in biochemical inhibitory assays (IC_{50} > 100 μM). Those results implied that **6g** might inhibit the phosphorylation of eIF4E in a different way with

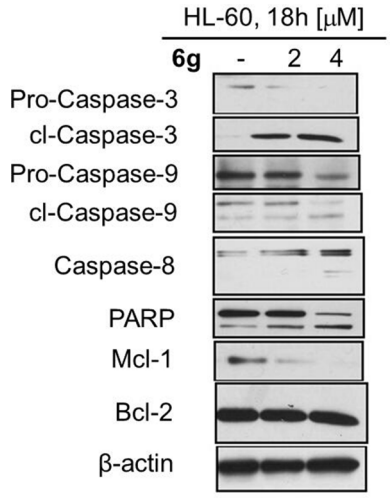

Fig. 4. 6g caused caspase activation and PARP cleavage. HL-60 cells were treated with 6g at indicated concentrations for 18 h.

its natural analogue Cercosporamide, which seemed to be the results of structure differences between them.

2.2.5. *6g exhibited potent pan-Pim kinases inhibitory activities*

eIF4E activity is indispensable for Pim-induced cap-dependent translation process, because Pim kinases, as well as c-myc, cyclin D1, Mcl-1, which are important in cell survival and cycle progression, rely on the eIF4E-mediated mechanism of translation. Pim kinases, a family of constitutively expressed and active serine/threonine kinases, are treated as potent oncogenes and overexpressed in a wide range of hematopoietic malignancies and solid cancers [24]. Pim kinases are highly expressed in acute myeloid leukemia and chronic myeloid leukemia, and Pim kinases exert its oncogenic activities through regulations of *myc*-driven transcription, 4E-BP1-involved cap-dependent translation and survival signaling through phosphorylation of Bcl-2-associated agonist of cell death (BAD) to lower the thresholds for apoptosis [25,26]. From this, it can be inferred that the apoptosis caused by compound **6g** may be due to inhibition of Pim kinases. In order to confirm the hypothesis, the effects on p-4E-BP1 and p-BAD were studied upon treatment of **6g** in K562 cells. As shown in Fig. 6, **6g**

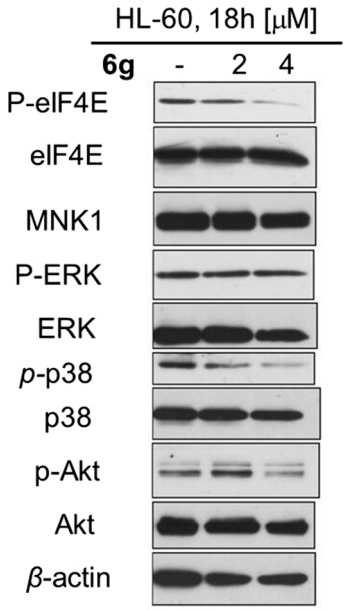

Fig. 5. 6g inhibited phosphorylation of eIF4E in leukemia cells. HL-60 cells were treated with 6g at indicated concentrations for 18 h. Cells were lysed for western blot analysis with specific antibodies.

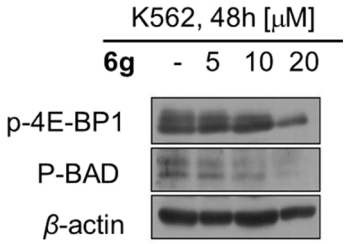

Fig. 6. 6g inhibited phosphorylation of 4E-BP-1 and BAD in K562 cells. K562 cells were treated with 6g at indicated concentrations for 48 h. Cells were lysed for western blot analysis with specific antibodies.

treatment decreased the expression of p-4E-BP1 and p-BAD, indicating the inhibition of Pim kinases in K562 cells.

To confirm the inhibitory effect of **6g** towards Pim kinases, direct kinase assay was performed. As shown in Table 2, **6a–6g** exhibited potent Pim inhibition; the inhibitory activities of 6a–6g against Pim-1 and Pim-3 are stronger than Pim-2, which is similar to most of the pan-Pim inhibitors. Compound **6g** exhibited the best kinases inhibitory activities with IC_{50} of 0.30 μM, 0.62 μM and 0.22 μM against Pim-1, Pim-2 and Pim-3 kinase, respectively. These results provide compelling evidence that the anti-proliferative activity of these compounds in HL-60 and K562 cell lines was mediated, at least in part, by the inhibition of Pim kinases. Furthermore, the proposed binding mode of **6g** with Pim-1 was studied using docking method, as can be seen from Fig. 7. Typically, ATP-competitive type-I kinase inhibitors form a pair of hydrogen bonds in the ATP-binding pocket of kinases, in a similar way to ATP. Pims kinases are the only kinases that cannot form the canonical bidentate hydrogen bonds with ATP and ATP competitive inhibitors because they have a proline residue in the hinge region at the position of the hydrogen donor. The lack of this hydrogen donor, a significant structural difference from other kinases, offers an opportunity to design Pims selective inhibitors. The predicted bonding mode demonstrated that **6g** completely entered and occupied the ATP binding pocket. No hydrogen bond with the hinge sequence of Pim-1 was established as expected. The *R*-methyl at C (9b) expanded to the small pocket formed by hydrophobic residues Arg122, Val126 and Leu174 and two hydrogen bond were established with Lys67 and Ile185, revealing a unique and tight binding manner. The data of *in vitro* kinase assays, effects on p-BAD and p-4E-BP1 together with proposed binding mode provided the first piece of evidence to support **6g** as a potential pan-Pim inhibitor.

Table 2
The Pim kinases inhibitory effects of compounds 6a-6 g.

Compd.	IC_{50}(μM)[a]		
	Pim-1	Pim-2	Pim-3
6a	0.42	2.45	0.56
6b	1.88	1.96	1.53
6c	1.21	8.22	1.08
6d	1.57	2.77	1.30
6e	2.14	6.41	2.00
6f	3.53	10.21	2.89
6g	0.30	0.62	0.22
(+)-UA	0.21	0.58	0.18

[a] Data shown are mean of duplicate experiments.

3. Conclusion

(+)-UA represents a promising lead for anticancer therapy. In this study, seven flavanone-based (+)-UA derivatives (**6a–6g**) were designed, synthesized and their anticancer activities were evaluated in leukemia cells. *In vitro* antiproliferative assay showed that **6a–6g** exhibited promising activities against HL-60 and K562 cells, the potency was improved by about 4-fold compared with (+)-UA. Further mechanism studies revealed that **6g** significantly induced leukemia cells apoptosis. Western blot assays indicated that **6g** suppressed the expression of Mcl-1, p-eIF4E in HL-60 cells. *In vitro* kinase assays demonstrated **6g** exhibited pan-Pim kinases inhibitory activity, molecular docking demonstrated a unique and tight binding between **6g** and Pim-1, together with effects of **6g** on p-BAD and p-4E-BP1 provided the first piece of evidence to support **6g** as a potential pan-Pim kinases inhibitor. In summary, our work elucidated the potential anticancer mechanism of (+)-UA derivative **6g**, suggesting **6g** as potential anti-leukemia compounds, and further evaluation of this kind of flavanone derivatives is on-going.

4. Experiments

4.1. Chemistry

Melting point was measured with X-4 digital micro melting point apparatus with temperature unrevised. Infra-red (IR) spectra were recorded on Bruker IR-27G spectrometer with KBr pellets. ^{1}H NMR spectra were measured with a Bruker ARX (400 MHz) spectrometer and ^{13}C NMR with a Bruker AV (100 MHz) instrument. Chemical shifts are recorded in δ units using tetramethylsilane as the standard (NMR peak description: s, singlet; d, doublet; t, triplet; q, quartet; m, multiplet; br, broad peak). Low resolution mass spectrometry (MS) was recorded with an Agilent 1100 ion trap liquid chromatography-mass spectrometer. Organic solutions were dried over anhydrous $MgSO_4$ during workup. Column chromatography was carried out on TELEDYNE ISCO Combiflash Rf+ preparative liquid chromatograph. Silica gel 60 (200–300 mesh) and TLC were purchased from Qingdao Haiyang chemical Co. Ltd. All commercial reagents and solvents were used without further purification unless otherwise noted. The purity of the target compounds was > 95% as determined by HPLC.

4.1.1. General procedure of *6a–6g*

To a stirred solution of (+)-UA (0.34 g, 1 mmol) in methanol (20 mL) was added substituted benzaldehyde (1.5 mmol) and aqueous solution of KOH (0.09 g, 2 mmol). After 4–8 h under reflux, the mixture was cooled to room temperature and evaporated to dryness. The residue

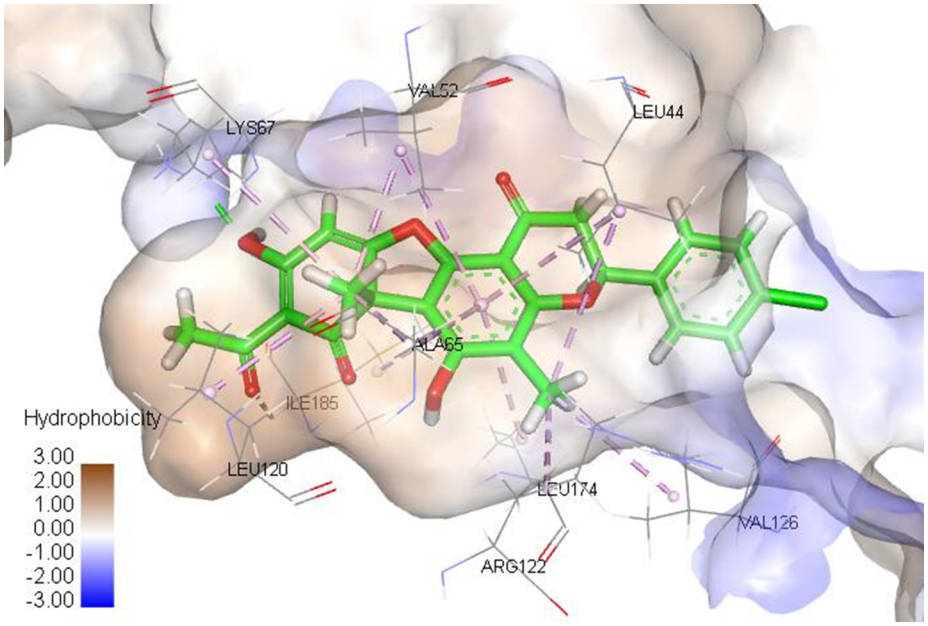

Fig. 7. The predicted binding mode of 6 g with Pim-1 (PDB 5DIA).

was re-dissolved with water (100 mL) and dichloromethane (100 mL). The organic layer was separated, washed with water and saturated brine, dried over sodium sulfate, concentrated and purified by column chromatography on silica (dichloromethane: methanol = 200:1). Subsequent HPLC was carried out for further purification (acetonitrile: water = 95:5) to give the title compound **6a–6g**.

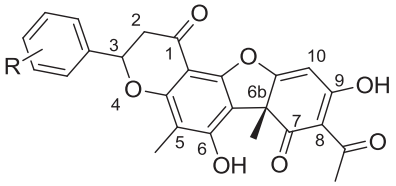

4.1.1.1. (6bR)-8-acetyl-6,9-dihydroxy-5,6b-dimethyl-3-phenyl-2,3-dihydro-1H-benzofuro[2,3-f]chromene-1,7(6bH)-dione ***(6a)***. Yellow solid; yield: 31%; M.p.:193.3–195.3 °C; IR (KBr, cm^{-1}) ν: 3424, 2922, 2852, 1678, 1619, 1603, 1541, 1459; LC-MS: 430.9 $[M-H]^-$; ^1H NMR ($CDCl_3$, 400 MHz): 11.15–11.09 (s, 1H, 6-OH), 7.38–7.50 (m, 5H, 2′3′4′5′6′ phenyl H), 6.08–6.07 (s, 1H, 10-H), 5.49 (dd, 1H, J = 2.8, 12.0 Hz, 3-H), 3.01 (dd, 1H, J = 4.0, 12.8 Hz, 2-H_{ax}), 2.90 (dd, 1H, J = 4.0, 16.8 Hz, 2-H_{eq}), 2.662–2.658 (s, 3H, 8-Ac), 2.160–2.156 (s, 3H, 5-Me), 1.76–1.75 (s, 3H, 6b-Me); ^{13}C NMR ($CDCl_3$, 100 MHz): 201.8, 198.1, 191.8, 189.1, 180.7, 161.2, 157.4, 153.8, 138.6, 128.8, 125.9, 110.1, 107.1, 105.1, 102.7, 98.7, 79.2, 58.8, 44.7, 44.4, 32.0, 28.0, 8.3.

4.1.1.2. (6bR)-8-acetyl-6,9-dihydroxy-5,6b-dimethyl-3-(3-nitrophenyl)-2,3-dihydro-1H-benzofuro[2,3-f]chromene-1,7(6bH)-dione ***(6b)***. Yellow solid; yield: 25%; M.p.: 164.1–166.1 °C; IR (KBr, cm^{-1}) ν: 3453, 2924, 1700, 1630, 1557, 1458, 1383; LC-MS: 478.1 $[M+H]^+$; ^1H NMR ($CDCl_3$, 400 MHz): 11.19–11.13 (s, 1H, 6-OH), 7.41(d, 4H, J = 4.0 Hz, 2′4′5′6′ phenyl H), 6.09–6.08 (s, 1H, 10-H), 5.46 (dd,1H, J = 3.6, 12.0 Hz, 3-H), 2.97 (dd, 1H, J = 12.4, 16.4 Hz, 2-H_{ax}), 2.88 (dd, 1H, J = 3.6, 16.8 Hz, 2-H_{eq}), 2.662–2.658 (s, 3H, 8-Ac), 2.151–2.148 (s, 3H, 5-Me), 1.76–1.75 (s, 3H, 6b-Me).

4.1.1.3. (6bR)-8-acetyl-3-(4-fluorophenyl)-6,9-dihydroxy-5,6b-dimethyl-2,3-dihydro-1H-benzofuro[2,3-f]chromene-1,7(6bH)-dione ***(6c)***. Yellow solid; yield: 31%; M.p.: 156.4–158.2 °C; IR (KBr, cm^{-1}) ν: 3452, 2923, 1699, 1630, 1557, 1463, 1383; LC-MS: 451.1 $[M+H]^+$; ^1H NMR ($CDCl_3$, 600 MHz): 18.84–18.83 (s, 1H, 9-OH), 11.16–11.11 (s, 1H, 6-OH), 7.44–7.47 (m, 2H, phenyl H), 7.11–7.15 (m, 2H, phenyl H), 6.08–6.07 (s, 1H, 10-H), 5.46 (dd,1H, J = 3.0, 12.0 Hz, 3-H), 2.99 (dd, 1H, J = 3.0, 7.2 Hz, 2-H_{ax}), 2.87 (dd, 1H, J = 3.6, 16.8 Hz, 2-H_{eq}), 2.660–2.656 (s, 3H, 8-Ac), 2.147–2.144 (s, 3H, 5-Me), 1.76–1.75 (s, 3H, 6b-Me); ^{13}C NMR ($CDCl_3$, 125 MHz): 201.6, 197.8, 191.6, 188.6, 188.5, 180.2, 163.3, 161.7, 160.8, 157.3, 127.6, 115.5, 109.8, 106.8, 104.9, 102.3, 98.5, 78.4, 58.5, 44.5, 44.1, 31.9, 27.8, 7.9.

4.1.1.4. (6bR)-8-acetyl-6,9-dihydroxy-3-(4-methoxyphenyl)-5,6b-dimethyl-2,3-dihydro-1H-benzofuro[2,3-f]chromene-1,7(6bH)-dione ***(6d)***. Yellow solid; yield: 16%; M.p.: 184.6–185.6 °C; IR (KBr, cm^{-1}) ν: 3425, 2924, 2853, 1677, 1621, 1604, 1515, 1462; LC-MS: 463.1 $[M+H]^+$; ^1H NMR ($CDCl_3$, 400 MHz): 11.14–11.08 (s, 1H, 6-OH), 7.40 (q, 2H, J = 4.0 Hz, phenyl H), 6.96 (q, 2H, J = 4.0 Hz, phenyl H), 6.09–6.08 (s, 1H, 10-H), 5.43 (dd, 1H, J = 2.8 Hz, 3-H), 3.844–3.836 (s, 3H, phenyl 4′-Me), 3.03 (dd, 1H, J = 2.8 Hz, 14.0 Hz, 2-H_{ax}), 2.81 (dd, 1H, J = 3.2 Hz, 5.2 Hz, 2-H_{eq}), 2.660–2.655 (s, 3H, 8-Ac) 2.138–2.135 (s, 3H, 5-Me), 1.76–1.75 (s, 3H, 6b-Me); ^{13}C NMR ($CDCl_3$, 100 MHz): 201.8, 198.1, 191.8, 189.8, 180.7, 161.3, 159.8, 157.3, 153.7, 130.7, 127.5, 114.1, 110.0, 107.0, 105.1, 102.6, 98.6, 79.0, 58.8, 55.3, 44.2, 44.1, 32.1, 28.1, 8.2.

4.1.1.5. (6bR)-8-acetyl-3-(4-bromophenyl)-6,9-dihydroxy-5,6b-dimethyl-2,3-dihydro-1H-benzofuro[2,3-f]chromene-1,7(6bH)-dione ***(6e)***. Yellow solid; yield: 27%; M.p.: 112.4–113.1 °C; IR (KBr, cm^{-1}) ν: 3425, 2922, 2852, 1677, 1622, 1605, 1543, 1461; LC-MS: 511.0 $[M+H]^+$; ^1H NMR ($CDCl_3$, 400 MHz): 11.13 (s, 1H, 6-OH), 7.58 (d, 2H, J = 8.4 Hz, phenyl H), 7.37 (d, 2H, J = 8.4 Hz, phenyl H), 6.08 (s, 1H, 10-H), 5.43 (dd, 1H, J = 3.6 Hz, 12.8 Hz, 3-H), 2.85–3.01 (m, 2H, 2-H), 2.66 (s, 3H, 8-Ac), 2.14 (s, 3H, 5-Me), 1.75 (s, 3H, 6b-Me); ^{13}C NMR ($CDCl_3$, 100 MHz): 201.8, 198.1, 191.8, 188.5, 180.6, 160.9, 157.5, 153.8, 137.7, 132.0, 127.6, 122.6, 110.1, 107.3, 105.1, 102.6, 98.7, 78.6, 58.7, 44.6, 32.0, 28.0, 8.2.

4.1.1.6. (6bR)-8-acetyl-3-(3-chlorophenyl)-6,9-dihydroxy-5,6b-dimethyl-2,3-dihydro-1H-benzofuro[2,3-f]chromene-1,7(6bH)-dione ***(6f)***. Yellow solid; yield: 30%; M.p.: 112.0–113.2 °C; IR (KBr, cm^{-1}) ν: 3429, 2922, 2852, 1674, 1622, 1544, 1460; LC-MS: 467.1 $[M+H]^+$; ^1H NMR ($CDCl_3$, 400 MHz): 11.17–11.14 (s, 1H, 6-OH), 7.49 (q, 1H, J = 3.2 Hz, phenyl H), 7.36–7.37 (m, 3H, phenyl H), 6.09–6.08 (s,

1H, 10-H), 5.45 (dd, 1H, J = 3.6 Hz, 12.8 Hz, 3-H), 2.86–3.01 (m, 2H, 2-H), 2.663–2.660 (s, 3H, 8-Ac) 2.169–2.165 (s, 3H, 5-Me), 1.77–1.76 (s, 3H, 6b-Me); ^{13}C NMR ($CDCl_3$, 100 MHz): 201.8, 198.0, 191.8, 188.6, 180.5, 160.9, 157.4, 153.7, 137.2, 134.5, 129.1, 127.3, 110.0, 107.2, 105.1, 102.6, 98.7, 78.5, 58.7, 44.7, 32.0, 28.0, 8.3.

4.1.1.7. (6bR)-8-acetyl-3-(4-chlorophenyl)-6,9-dihydroxy-5,6b-dimethyl-2,3-dihydro-1H-benzofuro[2,3-f]chromene-1,7(6bH)-dione ***(6g)***. Yellow solid; yield: 36%; M.p.: 98.3–99.2 °C, IR (KBr, cm^{-1}) ν: 3426, 2923, 2853, 1677, 1622, 1604, 1545, 1460; LC-MS: 467.1 $[M+H]^+$; ^{1}H NMR ($CDCl_3$, 400 MHz): 11.19–11.13 (s, 1H, 6-OH), 7.42 (q, 4H, J = 4.0 Hz, 2′3′5′6′ phenyl H), 6.09–6.08 (s, 1H, 10-H), 5.46 (dd, 1H, J = 3.6 Hz, 12.0 Hz, 3-H), 2.85–3.01 (m, 2H, 2-H), 2.661–2.658 (s, 3H, 8-Ac) 2.15 (s, 3H, 5-Me), 1.77–1.76 (s, 3H, 6b-Me); ^{13}C NMR ($CDCl_3$, 100 MHz): 201.8, 198.0, 191.8, 188.6, 180.5, 160.9, 157.4, 153.7, 137.2, 134.5, 129.0, 127.3, 110.0, 107.2, 105.1, 102.6, 98.7, 78.5, 58.5, 44.7, 32.0, 28.0, 8.3.

4.2. Cell growth inhibition assays

Cells were seeded at 5×10^4 cells/mL and incubated with the indicated concentrations of test compounds in 24-wells plate for three days. After treatment, cells were suspended and 50 μL suspensions were mixed with equal volume of 0.4% solution of trypan blue gently. The total number of cells and dead ones were determined with the aid of a hemocytometer. Live cells were round and bright, while dead cells appeared blue. Growth-inhibitory ability of the compounds was calculated and expressed as the ratio of the cell number of treated cells to that of untreated sells. The experiment was repeated at least three times.

4.3. Quantitation of apoptotic cells

Apoptotic cells were determined by morphologic observation and fluorescence-activated cell sorting (FACS) analysis after staining with PI. Cells treated with different concentrations of **6g** were fixed with ice-cold 70% ethanol at a density of 1×10^5 cells/mL and treated with 1 mg/mL RNase for 30 min at 37 °C. PI was then added to a final concentration of 50 μg/mL and the DNA content was quantitated by flow cytometry with an excitation wavelength of 488 nm and an emission wavelength of 625 nm. Data were analyzed using CELLQuest software.

4.4. Western blot analysis

HL-60 and K562 cells were treated with **6g** for 18 h and 48 h, respectively. Protein extracts (30 μg) prepared with RIPA lysis buffer [50 mM Tris-HCl, 150 mM NaCl, 0.1% SDS, 1%NP-40, 0.5% sodium deoxycholate, 1 mM phenylmethylsulfonyl fluoride (PMSF), 100 μM leupeptin and 2 μg/mL aprotinin (pH 8.0)] were estimated by BCA kit and denatured on metal bath at 98 °C for 5 min. Samples were loaded onto 10% SDS PAGE and proteins resolved at constant voltage, then transferred to nitrocellulose membranes, which were stained with 0.2% Ponceau S red to assure equal loading and transfer. After blocking by 5% non-fat milk for 1 h, specific antibody to responding proteins and β-actin were incubated overnight at 4 °C. Then it was treated with appropriate HRP-linked secondary antibody and processed for further improved ECL detection.

4.5. Kinase assay

Inhibition of MNK1/2 and Pim-1/2/3 were measured by HTRF (Homogeneous Time Resolved Fluorescence) assay using Cisbio KinaseProfiler services. Hail-maximal inhibition (IC_{50}) values were calculated from 10-point dose–response curves (The doses are: 10000 nM, 5000 nM, 2500 nM, 1250 nM, 625 nM, 312.5 nM, 156.3 nM, 78.1 nM, 39 nM, 19.5 nM). Staurosporine and (+)-UA were used as positive control. Briefly, 0.67 ng of Pim-1/2/3 or 2.0 ng of MNK1/2 was incubated with different concentrations of test compounds in an 8 μL reaction mixture (1 μM substrate S3, 36.7 μM (Pims kinase) or 39.2 μM (Mnks kinase) ATP, 5 mM $MgCl_2$, 1 mM Dithiothreitol and 1 × KinEASE enzymatic buffer) for 50 min at room temperature. Reactions were terminated through adding 10 μL EDTA-containing detection reagents following the kit protocol. The ratio between the HTRF signals of 615 and 665 nm was recorded with an Infinite® F500 microplate reader (Tecan, Switzerland) and IC_{50} values were calculated from the inhibition curves.

4.6. Molecular modeling

Discovery studio 3.0 was used to perform in silico docking. The X-ray crystal structure of Pim-1 kinase in complex with the ligand [27] was retrieved from Protein Data Bank (PDB code 5DIA). All calculations and manipulations were performed with libdock modules in the Discovery studio software package. All water molecules were removed and hydrogen was added. By applying the default parameters, the best docking result was selected to analysis based on the favorable binding affinity rank in kcal/mol (docking score).

Acknowledgments

This work was supported by the National Natural Science Foundation of China (Grant No. 81773578).

References

[1] A.M.L. Seca, D.C.G.A. Diana, Plant secondary metabolites as anticancer agents: successes in clinical trials and therapeutic application, Int. J. Mol. Sci. (2018) 263/1–263/22.
[2] K. Ingolfsdottir, Usnic acid, Phytochemistry 61 (2002) 729–736.
[3] A.A.S. Araujo, M.G.D. de Melo, T.K. Rabelo, P.S. Nunes, S.L. Santos, M.R. Serafini, et al., Review of the biological properties and toxicity of usnic acid, Nat. Prod. Res. 29 (2015) 2167–2180.
[4] M.A. Bazin, A.C.L. Lamer, J.G. Delcros, I. Rouaud, P. Uriac, J. Boustie, et al., Synthesis and cytotoxic activities of usnic acid derivatives, Bioorgan. Med. Chem. 16 (2008) 6860–6866.
[5] B.W. Konicek, J.R. Stephens, A.M. McNulty, N. Robichaud, R.B. Peery, C.A. Dumstorf, et al., Therapeutic inhibition of MAP kinase interacting kinase blocks eukaryotic initiation factor 4E phosphorylation and suppresses outgrowth of experimental lung metastases, Can. Res. 71 (2011) 1849-1857.
[6] M.A. Conover, R. Mierzwa, A. King, D. Loebenberg, W.R. Bishop, M. Puar, et al., Usnic acid amide, a phytotoxin and antifungal agent from *Cercosporidium henningsii*, Phytochemistry 31 (1992) 2999–3001.
[7] S. De Lombaert, L. Blanchard, L.B. Stamford, J. Tan, E.M. Wallace, Y. Satoh, et al., Potent and selective non-peptidic inhibitors of endothelin-converting enzyme-1 with sustained duration of action, J. Med. Chem. 43 (2000) 488–504.
[8] D.N. Sokov, V.V. Zarubaev, A.A. Shtro, M.P. Polovinka, O.A. Luzina, N.I. Komarova, Anti-viral activity of (-)- and (+)-usnic acids and their derivatives against influenza virus A(H1N1)2009, Bioorg. Med. Chem. Lett. 22 (2012) 7060–7064.
[9] M. Bruno, B. Trucchi, B. Burlando, E. Ranzato, S. Martinotti, E.K. Akkol, et al., (+)-Usnic acid enamines with remarkable cicatrizing properties, Bioorg. Med. Chem. 21 (2013) 1834–1843.
[10] M. Bruno, B. Trucchi, D. Monti, S. Romeo, M. Kaiser, L. Verotta, Synthesis of a potent antimalarial agent through natural products conjugation, ChemMedChem 8 (2013) 221–225.
[11] Y. Song, F. Dai, D. Zhai, Y. Dong, J. Zhang, B. Lu, et al., Usnic acid inhibits breast tumor angiogenesis and growth by suppressing VEGFR2-mediated AKT and ERK1/2 signaling pathways, Angiogenesis 15 (2012) 421–432.
[12] N. Singh, D. Nambiar, K. Raosaheb, R.P. Singh, Usnic acid inhibits growth and induces cell cycle arrest and apoptosis in human lung carcinoma A549 cells, Nutr. Can. 65 (2013) 36–43.
[13] S. Zuo, L. Wang, Y. Zhang, D. Zhao, Q. Li, D. Shao, et al., Usnic acid induces apoptosis via an ROS-dependent mitochondrial pathway in human breast cancer cells in vitro and in vivo, RSC Adv. 5 (2014) 153–162.
[14] Y. Fan, M. Huang, Y. Cao, P. Gong, W. Liu, S. Jin, et al., Usnic acid is a novel Pim-1 inhibitor with the abilities of inhibiting growth and inducing apoptosis in human myeloid leukemia cells, RSC Adv. 6 (2016) 24091–24096.
[15] R.J. Ferreira, R. Baptista, A. Moreno, P.G. Madeira, R. Khonkarn, H. Baubichon-Cortay, et al., Optimizing the flavanone core toward new selective nitrogen-containing modulators of ABC transporters, Future Med. Chem. 10 (2018) 725–741.
[16] P. Srivarangkul, W. Yuttithamnon, S. Pankaew, A. Suroengrit, K. Hengphasatporn, T. Rungrotmongkol, et al., A novel flavanone derivative inhibits dengue virus fusion and infectivity, Antivir. Res. 151 (2018) 17–38.
[17] D.N. Sokolov, O.A. Luzina, M.P. Polovinka, N.F. Salakhutdinov, G.A. Tolstikov,

Russ. Chem. B+. 60 (2011) 2406–2411.
[18] D.N. Sokolov, M.E. Rakhmanova, O.A. Luzina, A.V. Shernyukov, N.F. Salakhutdinov, Synthesis of chalcones derived from (+)- and (-)-usnic acids, Russ. Chem. B+. 62 (2013) 212–216.
[19] S. Bano, K. Javed, S. Ahmad, I.G. Rathish, S. Singh, M. Chaitanya, et al., Synthesis of some novel chalcones, flavanones and flavones and evaluation of their anti-inflammatory activity, Eur. J. Med. Chem. 65 (2013) 51–59.
[20] O.A. Luzina, D.N. Sokolov, A.V. Shernyukov, N.F. Salakhutdinov, Synthesis of aurones based on usninic acid, Chem. Nat. Compd+. 48 (2012) 385–391.
[21] A.B. Dincsoy, D. Cansaran, Demet, Changes in apoptosis-related gene expression profiles in cancer cell lines exposed to usnic acid lichen secondary metabolite, Turk. J. Biol. 41 (2017) 484–493.
[22] Y. Kiraz, A. Adan, M. Kartal Yandim, Y. Baran, Major apoptotic mechanisms and genes involved in apoptosis, Tumor Biol. 37 (2016) 8471–8486.
[23] M. Bhat, N. Robichaud, L. Hulea, N. Sonenberg, J. Pelletier, I. Topisirovic, Targeting the translation machinery in cancer, Nat. Rev. Drug discov. 14 (2015) 261–278.
[24] Y. Sawaguchi, R. Yamazaki, S. Yukiko, T. Sasai, M. Mae, A. Abe, et al., Rational design of a potent pan-pim kinases inhibitor with a rhodanine-benzoimidazole structure, Anticancer Res. 37 (2017) 4051–4057.
[25] M.E. Abdelaziz, M.M.M. Mostafa, S.M. Salwa, M.A. Mahran, A.A. Hazzaa, Design, synthesis and docking study of pyridine and thieno[2,3-b] pyridine derivatives as anticancer PIM-1 kinase inhibitors, Bioorg. Chem. 80 (2018) 674–692.
[26] N.A. Keane, M. Reidy, A. Natoni, M.S. Raab, M. O'Dwyer, Targeting the Pim kinases in multiple myeloma, Blood Cancer J. 5 (2015) e325.
[27] H.H. Wang, Discovery of 3,5-substituted 6-azaindazoles as potent pan-Pim inhibitors, Bioorg. Med. Chem. Lett. 25 (2015) 5258–5264.